Computer simulation of granular shear flows

By CHARLES S. CAMPBELL†

AND CHRISTOPHER E. BRENNEN

Division of Engineering and Applied Science, California Institute of Technology,
Pasadena, CA 91125

Detailed understanding of flowing granular materials is severely hampered by the deficiencies of present experimental methods. To help increase the information base, a computer simulation has been developed to describe two-dimensional unidirectional flows of inelastic fully rough particles. This paper presents the results of a Couette shear-flow simulation. The results include distributions of velocity, density and granular temperature (a measure of the kinetic energy contained in the random particle motions). The effects of density and shear rate on the granular temperature are explored. Shear and normal forces on the solid walls are compared with experimental and theoretical results. The behaviour of the particles in the simulated flow is examined and assessments are made of the collision angle and velocity distributions. The development of a distinct, 'layered' microstructure is observed in high-density granular flows.

1. Introduction

The particles composing a static granular material interact at interparticle contact points. A granular material will behave like a solid as long as the forces on the bulk material are supported across the contact points. While the frictional bonds hold bulk-material deformation is accomplished by elastic deformation of the constituent particles. When the interparticle bonds are broken the particles are free to move relative to one another and the bulk material will deform plastically. A bond breaks when the force tangential to the particle at the point of contact exceeds a certain fraction of the normal force. Plastic deformation can occur under a large variety of stress loadings. For low normal stress the strength of the tangential bonds will be weak and the material may deform and flow like a fluid under very small shear loadings.

Much recent work has been devoted to understanding the mechanical properties of flowing granular materials and certain limiting granular-flow regimes have been identified. The 'quasistatic' flow regime occurs at extremely low strain rates when particles remain in contact for long periods of time. The current state of knowledge has been recently reviewed by Spencer (1981) and Mroz (1980). At the other end of the spectrum is the 'rapid-flow' or 'grain-inertia' regime, which occurs at very high shear rates. In this regime the inertia associated with the relative motions of the particles becomes significant and the particles may be assumed to interact by instantaneous collisions rather than by long-term frictional sliding at particle contact points. The collisions induce random instantaneous particle velocities. Thus, associated

---

† Present address: Department of Mechanical Engineering, University of Southern California, Los Angeles, CA 90089-1453.

with the mean velocity field is a field of random particle velocities reminiscent of the thermal motions of particles in a gas or liquid. The energy associated with the random motions is often referred to as the 'granular temperature', or simply the temperature of the flow. Granular materials in the grain-inertia regime are similar to hard-sphere models of gases, and many recent theoretical works (Blinowski 1978; Kanatani 1979a,b, 1980; Ogawa & Oshima 1977; Ogawa 1978; Oshima 1978, 1980; Savage & Jeffrey 1981; Ackermann & Shen 1982; Jenkins & Savage 1983) are based on molecular models of non-equilibrium gas flows (see Chapman & Cowling 1970; Ferziger & Kaper 1972). In fact, the hard-sphere approximation is more appropriately applied to granular interactions than molecular interactions. The major differences are that granular flows occur at much higher densities than are ever likely to be encountered in gases, and that granules collide inelastically. The state of knowledge in the rapid-flow regime has recently been reviewed by Savage (1984).

The gaps between particles will generally be filled with an interstitial fluid. In both the quasistatic and grain-inertia regimes all effects of the interstitial fluid have been neglected in determining the flow behaviour. This assumes that the particle–particle interactions dominate the particle–fluid interactions. At extremely low densities particle–particle interactions are infrequent and the fluid–material combination acts like a fluid with some viscosity correction to account for the presence of the particles. (This has been dubbed the 'macroviscous regime' by Bagnold (1954).) The first analysis that led to a form of the corrected viscosity was performed by Einstein (1906). The conditions have not been well defined under which interstitial-fluid effects may be neglected in determining the mechanical behaviour of the material and a long discussion of this problem appears in Savage (1984).

Granular-material flows lend themselves to computer simulation. While the behaviour of the bulk material is not well understood, the individual particle interactions – surface friction and particle collisions – are easily described by simple analytical expressions. If interstitial-fluid effects can be neglected, there are no long-range forces between the particles, and all particle interactions occur at particle–particle contact points. Then, between contacts, a particle may be assumed to follow a kinematic trajectory described by a simple algebraic function of time. Based on the laws of particle interactions and trajectories, a computer simulation may be built that mechanistically follows individual particles, within an assemblage, as they interact with other particles and the system's boundaries. The simulation describes the instantaneous 'state' of the system, which is completely given by the instantaneous positions and velocities of the constituent particles. From that knowledge, any information about the system can be obtained. In particular, the 'continuum' information – velocity, density and temperature profiles – may be determined by averaging over instantaneous system states. In effect an experiment is performed on the computer: a mechanical system is set up and measurements are made upon it. The validity of the results depends on how accurately the individual particle interactions are approximated.

Computer models of granular materials have been developed by Cundall (1974), Davis & Deresiewicz (1977), Cundall & Strack (1979), Trollope & Berman (1980) and Walton (1980, 1982a,b). All but the last have been applied to small, mostly elastic, deformation of granular structures. (Cundall (1974) used simulations of a rockslide and the filling and emptying of a hopper to illustrate the versatility of his program, but did not pursue the investigations in any detail.) Walton's model, developed at the Lawrence Livermore Laboratory, was used to produce ciné films of large-deformation flows of arbitrarily shaped particles. To our knowledge, none of these simulations has been used for the determination of basic granular-flow properties.

The purpose of the present work is to produce a computer simulation of rapid granular flows that may be used to examine the detailed behaviour of the system. The simulation was designed to run efficiently, allowing a large number of flow parameters to be varied within the means of limited computer resources. Towards that end, only two-dimensional flows of two-dimensional disks or cylinders were modelled. There is nothing in the simulation scheme that prevents the modelling of three-dimensional flows of three-dimensional particles, except that the greater number of particles required to fill a similar-sized system would greatly increase the computational costs. We felt that a large number of two-dimensional simulations would better serve the limited state of knowledge of granular systems than a few three-dimensional simulations. Geometrically simple unidirectional flows were simulated to facilitate both the execution of the simulation and the interpretation of the results. The gravity-free flow in a Couette shear cell and the gravity-driven flow down an inclined chute have been modelled. (The results of the chute simulation appear in Campbell (1982) and Campbell & Brennen (1982b, 1984).) Both are particularly useful systems. The simple chute flow illustrates many relatively complicated features while the Couette flow is relatively simple and allows detailed examination of many general features of granular flows. Both have been the subject of numerous experimental and theoretical studies. In particular, the Couette-flow experiments of Bagnold (1954), Savage (1979) and Savage & Sayed (1980, 1983) are the only sources of knowledge of the constitutive behaviour of granular flows.

Three levels of understanding may be obtained from the simulation. The first is an observation of the phenomenological behaviour of granular flows such as the shapes of velocity and density profiles. Insight may also be obtained into the constitutive behaviour of the bulk material. In both cases the information may be compared with the limited experimental and theoretical results that are now available. Finally the simulation is used to gain some insight into the microstructural (particle-level) behaviour of granular systems. It is unlikely that experimental techniques will be developed to the point that is possible to make measurements on the microscale, although that information is easily accessible to a computer simulation.

A preliminary report of this work may be found in Campbell & Brennen (1982a). A short animated film has been prepared from a few of the simulated systems.

2. Computer simulation

A detailed account of the computer simulation is given in Campbell (1982) and will only be briefly repeated here.

Throughout the simulation, the particles (of mass m and radius R) are confined within a control volume. A schematic of the control volume is shown in figure 1 and several snapshots drawn from the simulation are shown in figure 2. For the Couette-flow simulation both the top and bottom of the control volume are closed by solid boundaries. (In the chute-flow simulation only the bottom is closed by a solid boundary; the top is left unbounded to simulate a free surface.) The solid walls are separated by a distance H and the upper wall is given a velocity U in the x-direction relative to the bottom wall. The sides of the control volume are bounded by 'periodic' boundaries: as a particle passes through one periodic boundary it reenters the other with exactly the same position and relative velocity with which it left. (This type of boundary is called 'periodic' because it emulates a situation in which the entire control volume is periodically repeated infinitely many times upstream and downstream.) This set-up greatly enhances the computational efficiency of the simulation
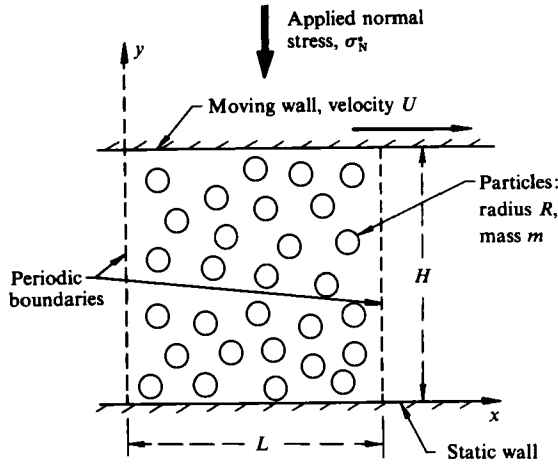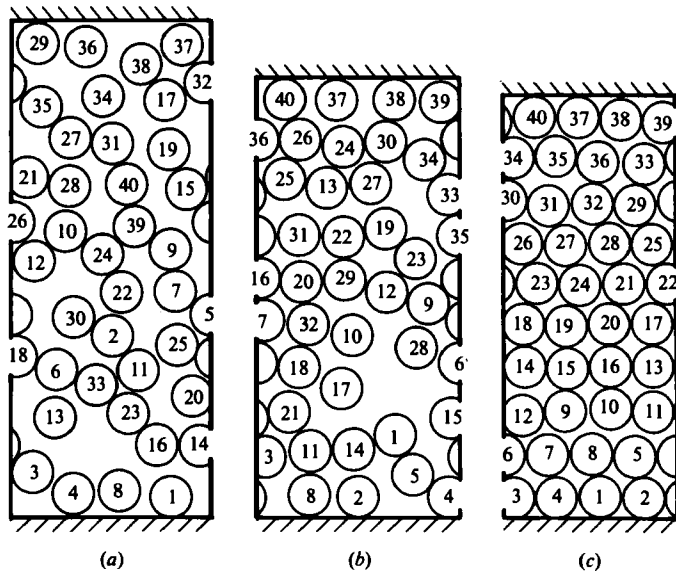
FIGURE 1. Schematic of the Couette-flow simulation.

FIGURE 2. Typical snapshots of the Couette-flow simulation: (a) $v = 0.56$; (b) 0.63; (c) 0.76.

by limiting the number of particles to those initially placed in the control volume. It has the drawback that it is only applicable to flows with no gradients in the flow direction (steady unidirectional flows). The separation L between the periodic boundaries was chosen so that further lengthening did not significantly alter the results of a few typical simulations.

Each simulation is begun with the particles arranged in a randomly perturbed square lattice. The initial translational velocities (u, v in the x-, y-directions of figure 1) and angular rotational velocity ω (measured positive in the counterclockwise direction) were chosen to be random perturbations about the continuum-fluid solution ($u(y) = Uy/H$, $v = \omega = 0$). From the initial configuration, each particle's trajectory is followed as it collides with the other particles and the boundaries of the control volume.

The first simulations were performed with the solid walls maintained at a fixed distance H apart. With this stipulation, the bulk of particles soon lost contact with the walls and travelled like a plug down the centre of the channel. In the present configuration the walls move in order to insure contact with the particles. A normal stress σ_N^* is specified as an input parameter to the program. Short-time averages of the normal impulses applied by the particles to the wall are compared with σ_N^*, and the walls are moved in or out accordingly.

The simulation is allowed to proceed until it converges to a steady state. Attainment of a converged state must be determined from some instantaneously observable parameters. For the Couette simulation a converged state occurred when the total system kinetic energy and the solid-wall spacing achieve nearly constant values. The determination of convergence is hindered because both parameters fluctuate slightly. Such fluctuations are to be expected in small thermodynamic systems (see Landau & Lifshitz 1958). Also, the Couette-flow experiments of Savage & Sayed (1983) showed similar fluctuations of the measured shear and normal stresses on the moving walls. For most of the Couette-flow calculations, convergence was achieved after as little as 500 collisions per particle from the initial state. (Some of the chute-flow calculations took as long as 5000 collisions per particle to converge.)

Once the system has converged, continuum-flow properties are obtained by averaging over successive instantaneous states of the system. The vertical span of the control volume is divided into strips parallel to the solid walls. At each sampling, the properties of the particles inside each strip are averaged. If a particle only partially occupies a strip, the averaging is weighted by the fraction of the particle that resides within the strip. These instantaneous averages are themselves averaged over many sampling times – for periods as long as 500 collisions per particle. The average value of a property p determined in this way is denoted $\langle p \rangle$.

Each particle collision is assumed to occur instantaneously once the particle surfaces have come into contact. (This is essentially the hard-sphere approximation). The collision result is computed from the standard centre-of-mass collision solution. Because the particles rotate as well as translate, two conditions are required to close the system of equations; one for the relative particle velocities normal to the particle surfaces at contact and the other for the particle velocities tangential to the surface at the contact point. The normal-velocity condition assumes that the particles are nearly elastic in the sense that energy is dissipated as a result of the collision but the particles involved do not deform. This is realized through a coefficient of restitution ϵ_p ($\epsilon_p < 1$), which is the ratio of the approach to recoil velocities in the centre-of-mass system and is specified as an input parameter to the program. The tangential-velocity condition assumes that on departure, after a collision, there will be zero relative tangential velocity between the surfaces of the particles. This will be called a 'fully rough' surface condition, as it corresponds to an infinite surface-friction angle; it should not be confused with the artificial rough-surface conditions used in kinetic-theory models of gases which do not dissipate energy. In this case, both the normal and tangential conditions result in energy dissipation.

The ratio of the approach to recoil velocities in a particle–wall collision is also given by a coefficient of restitution ϵ_ω, which may be specified independently of ϵ_p. Two different tangential-velocity conditions were applied. As for particle–particle collisions, the type-A wall condition assumes that the wall surface is fully rough in the sense that after a collision there is zero relative tangential slip between the particle surface and the wall. The type-B wall condition is an attempt to approximate a classical no-slip condition by assuming that after a wall collision the particle centre assumes the same

tangential velocity as the wall with no change in its rotation rate. This is felt to be similar to the conditions found in the Couette-flow experiments of Bagnold (1954) and Savage & Sayed (1980, 1983) in which the walls were roughened by particles glued to the wall surfaces.

The coefficients of restitution ϵ_w and ϵ_p are the only material properties that appear in the simulation. The distribution of mass within the particle may be specified by β, the square of the ratio of the particle's radius of gyration to its radius. Throughout the simulation, $\beta = 0.5$, the value appropriate for solid cylinders, is used.

Other than the properties ϵ_w, ϵ_p and β, the collision equations depend only on the particle mass m and the particle radius R. A timescale enters the problem only through the upper-wall velocity U. The only other lengthscale of importance is the separation H of the solid walls. (The separation L of the periodic boundaries is deliberately chosen long enough so as not to be of importance.) The results of the Couette-flow simulation will be presented non-dimensionally by dividing the velocities by the upper-wall velocity U, lengths by R or H, densities by the particle density $m/\pi R^2$ (the dimensionless density $\nu = \rho\pi R^2/m$ is known as the 'solid fraction') and stresses by mU^2/R^3. The only parameters that affect the results are (i) the ratio R/H of particle radius to wall spacing, (ii) the dimensionless normal stress $\sigma_N = \sigma_N^* R/mU$ and (iii) the dimensionless material properties ϵ_p, ϵ_w and β.

3. Velocity, solid-fraction and temperature profiles

Typical velocity, density and granular-temperature profiles for the type-A (rough wall surface) flows are shown in figure 3 for $\epsilon_w = 0.8$, $\epsilon_p = 0.6$ and various values of the dimensionless normal stress σ_N. The data are plotted as functions of the distance y measured from the lower stationary wall to the upper moving wall. These velocity profiles are characteristic of all such simulations. At either wall there is a slip of about 20–25 % of the upper-wall velocity. The flow shears all the way across its depth, but shows a region of particularly large shear next to both solid walls. The solid-fraction profiles all have a central region of relatively constant density and regions of decreasing density towards each solid wall. These results are consistent with the type-A chute-flow simulations reported in Campbell & Brennen (1984).

The last graph, labelled 'temperature', plots a measure of the kinetic energy contained in the random particle motions. The mean square of the fluctuation of a property p is denoted by $\langle p'^2 \rangle$; denoting the mean-square value of p by $\langle p^2 \rangle$ and the square of the mean value of p by $\langle p \rangle^2$, $\langle p'^2 \rangle$ may be written:

$$\langle p'^2 \rangle = \langle p^2 \rangle - \langle p \rangle^2. \tag{1}$$

The total temperature T is defined as twice the energy, per unit mass, associated with the particle fluctuations:

$$T = \langle u'^2 \rangle + \langle v'^2 \rangle + \beta R^2 \langle w'^2 \rangle. \tag{2}$$

Temperature is a byproduct of interparticle collisions. In a static granular material, any temperature would be quickly dissipated by the inelastic collisions. Thus temperature can be maintained only when driven by gradients in the mean velocity field. It can be clearly seen in figure 3 that the temperature is low across the central portion of the flow and large in the high-shear-rate regions next to each solid boundary. The high-temperature zones also correspond to the low-density regions. Campbell & Brennen (1984) have shown that the density appears to obey a heuristically proposed equation of state based on this temperature.
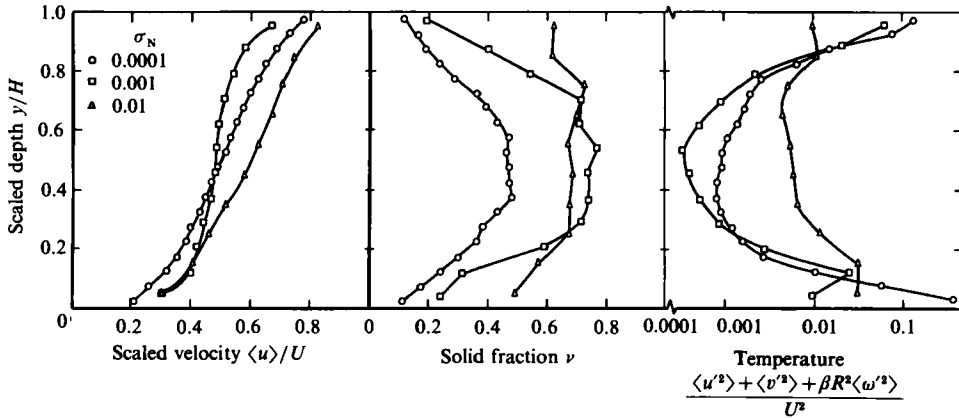
FIGURE 3. Typical velocity, solid-fraction and temperature profiles for the type-A Couette-flow simulation, $\epsilon_w = 0.8$, $\epsilon_p = 0.6$. Data are shown for $\sigma_N = 0.0001$ and $R/H = 0.025$, $\sigma_N = 0.001$ and $R/H = 0.042$ and $\sigma_N = 0.01$ and $R/H = 0.051$.
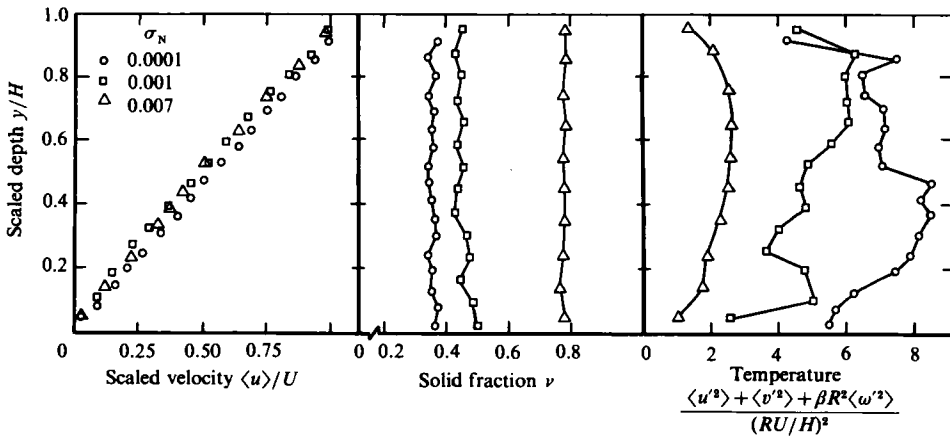

FIGURE 4. Typical velocity, solid fraction and temperature profiles for the type-B Couette-flow simulations, $\epsilon_w = 0.8$, $\epsilon_p = 0.6$. Data are shown for $\sigma_N = 0.0001$ and $R/H = 0.025$, $\sigma_N = 0.001$ and $R/H = 0.034$, $\sigma_N = 0.007$ and $R/H = 0.048$. Note that the temperature has been scaled by dividing by $(R/H)^2$.

Typical type-B (no-slip) Couette-flow results are presented in figure 4 for three different normal stresses σ_N. The velocity profiles show no slip at either wall, and vary linearly, with constant shear rate, from the stationary lower wall to the moving upper wall. The solid fraction is virtually uniform across the depth, and increases with increasing normal stress loads. For reasons to be discussed below, the temperatures shown here have been scaled by dividing by $(R/H)^2$. As would be expected, the temperatures are also roughly uniform across the depth. (The scatter in the temperature profiles at low densities is amplified by dividing by the square of an extremely small R/H.) In general the ratio of temperature to $(R/H)^2$ can be seen to decrease with increasing σ_N and the consequent increase in ν. (Note that the temperature in figure 4 is plotted on a linear scale, while that in figure 3 is plotted on a log scale.)

Surprisingly, the low-density high-shear-rate zones near the walls that appear in the type-A simulations are absent from the type-B simulations, indicating that the
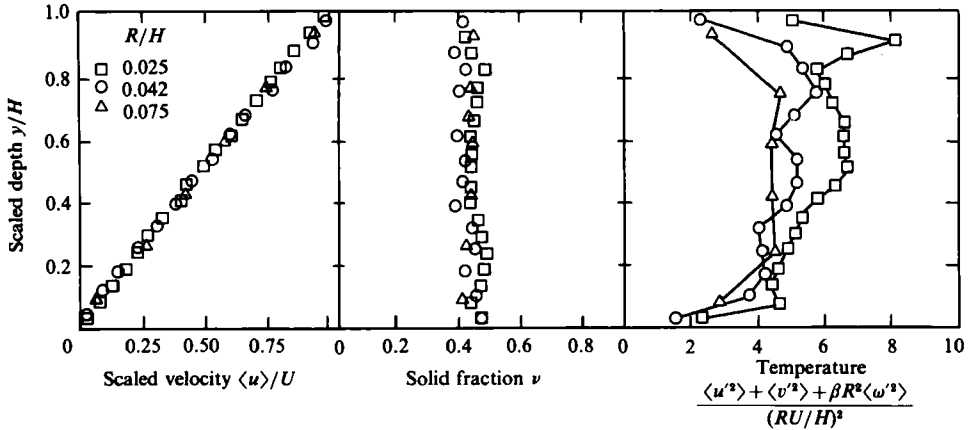
FIGURE 5. Comparison of type-B simulation results for different values of R/H, $\epsilon_w = 0.8$, $\epsilon_p = 0.6$, all with the normal stress varied as $\sigma_N = 0.567(R/H)^2$. Note that the temperature has been scaled by dividing by $(R/H)^2$.

behaviour of the flow, near solid boundaries, is strongly influenced by the wall boundary condition. Heuristically, this effect may be attributed to the large rotational impulse that is applied to the particle on collision with a type-A wall. On subsequent collisions with other particles, the rotational momentum will be transferred, in part, to random linear momentum, causing a rise in the local temperature and a decrease in the local solid fraction. Simulations with the type-B wall condition produce uniform shear flows, and, although it is a somewhat artificial boundary condition, it provides an opportunity to examine the detailed constitutive and microstructural behaviour of granular systems under controlled conditions. The rest of this paper will deal exclusively with type-B simulations.

A series of simulations was run to test the effect of varying R/H on the flow properties. The value of R/H is varied by changing the number of particles in the control volume while keeping the width L fixed. To hold the density constant, the dimensionless normal stress is varied as the square of R/H according to the rule

$$\sigma_N = \frac{\sigma_N^*}{\rho_p R^2 U^2} = 0.567 \left(\frac{R}{H}\right)^2. \tag{3}$$

(This relation implies $\sigma_N^* \propto \rho_p R^2 (U/H)^2$, and was chosen to be consistent with the results of the Couette-flow experiments of Bagnold (1954) and Savage & Sayed (1980, 1984). These will be discussed in greater detail in §5. The value 0.567 was chosen to correspond to the $\sigma_N = 0.001$ simulation shown in figure 4.) It can be seen in figure 5 that, as expected, the density is independent of R/H when the stress is varied in the prescribed manner. Note that the ratio of the temperature to the square of the velocity gradient has roughly the same value for all three shear rates. This indicates that, at constant density and for fixed particle radius R, the temperature varies as $(U/H)^2$, the square of the global velocity gradient. This is a special case, however, because there are only small gradients in the local temperature. Campbell & Brennen (1982b, 1984) present an example where the temperature is non-zero inside a non-shearing plug. In that case the temperature appears to be conducted into the plug from the surrounding high-temperature zones. If large temperature gradients are present, such as those found in the type-A simulations, conduction effects would
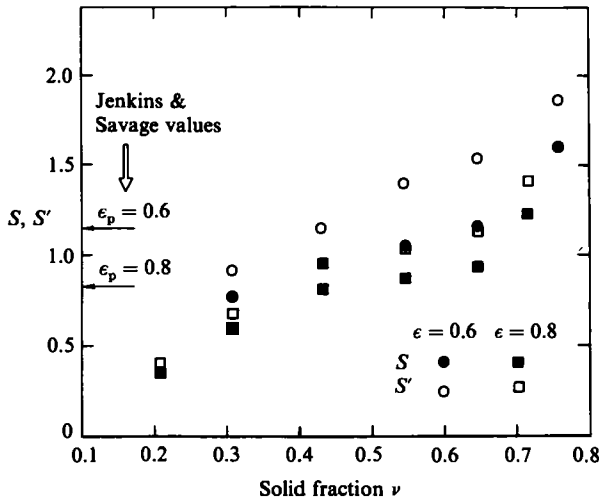
FIGURE 6. Parameters S and S' as functions of ν for type-B Couette-flow simulations, $\epsilon_w = 0.8$.

have to be taken into account, and the temperature would not be directly proportional to the square of the local velocity gradient.

The ratio of the shear rate to temperature may be represented by a dimensionless quantity S:

$$S = \frac{2R\,|\,\mathrm{d}u/\mathrm{d}y\,|}{(\langle u'^2 \rangle + \langle v'^2 \rangle + \beta R^2 \langle w'^2 \rangle)^{\frac{1}{2}}} = \frac{2R\,|\,\mathrm{d}u/\mathrm{d}y\,|}{T^{\frac{1}{2}}}. \tag{4}$$

The local values of a similar quantity S' relating the velocity gradient to that component of temperature associated with the translational velocities u and v,

$$S' = \frac{2R\,|\,\mathrm{d}u/\mathrm{d}y\,|}{(\langle u'^2 \rangle + \langle v'^2 \rangle)^{\frac{1}{2}}}, \tag{5}$$

play an important role in the constitutive models of Savage & Jeffrey (1981) and Jenkins & Savage (1983). (Rotations do not appear in their calculations because they assume completely smooth particles.) A plot of the average values of S as a function of solid fraction is shown in figure 6. The set of data is derived from type-B simulations with two particle coefficients of restitution. The corresponding values of S' are included to compare with the predicted values of Jenkins & Savage (1983). Jenkins & Savage predict that S' will be independent of the density and depend only on the coefficient of restitution. The simulation results show that both S and S' are increasing functions of density.

Figure 7 shows the partition of temperature into its components $\langle u'^2 \rangle$, $\langle v'^2 \rangle$ and $\beta R^2 \langle w'^2 \rangle$ as a function of solid fraction ν. This set of data is derived from simulations with $\epsilon_w = \epsilon_p = 0.8$, although similar behaviour is seen for other coefficients of restitution. The plotted values have been scaled by dividing by the squared shear rate. The scaled values of all three components decrease with solid fraction. In almost all cases, $\langle u'^2 \rangle / (UR/H)^2$ has the greatest and $\beta \langle w'^2 \rangle / (U/H)^2$ has the smallest value.

Figure 8 shows the distribution of the angular rotation rate $\langle w \rangle$ across the flow depth. The measured values are taken from the same simulations as figure 4, and have been scaled by dividing by U/H. The values of $\langle w \rangle$ are scattered about a mean value of roughly $-U/2H$. Recent calculations by one of the authors (Campbell 1984)
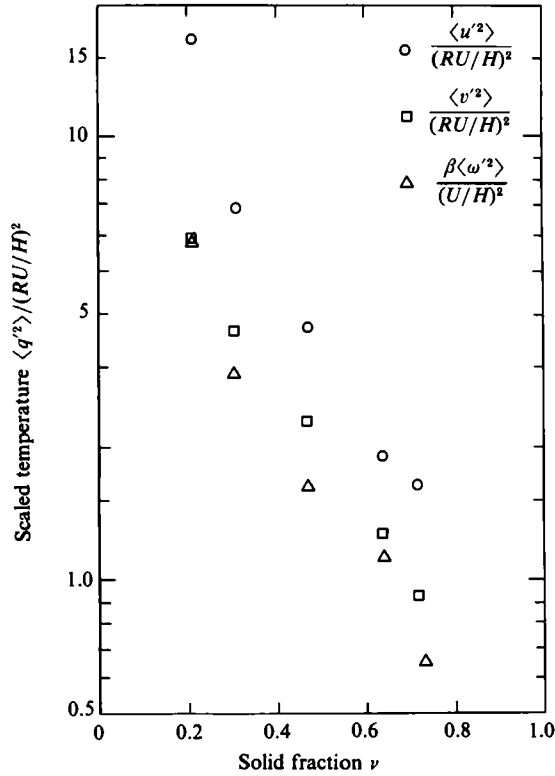
FIGURE 7. Scaled partition of temperature into its three components $\langle u'^2 \rangle/(UR/H)^2$, $\langle v'^2 \rangle/(UR/H)^2$ and $\beta R^2 \langle w'^2 \rangle/(U/H)^2$ as functions of v for type-B Couette-flow simulations, $\epsilon_w = \epsilon_p = 0.8$.
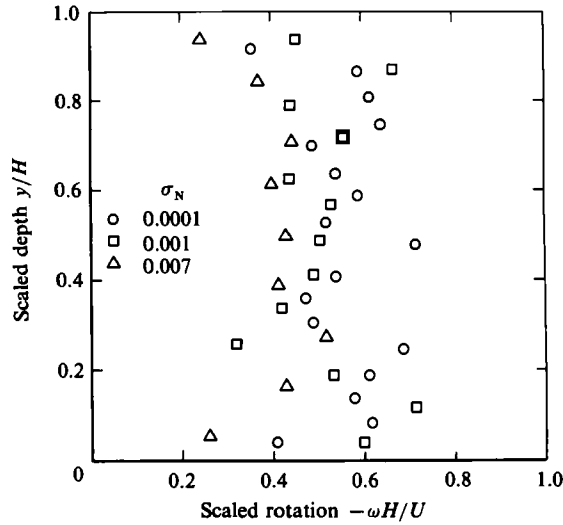

FIGURE 8. Distribution of scaled angular velocity $-\omega H/U$ for type-B Couette-flow simulations, $\epsilon_w = 0.8$, $\epsilon_p = 0.6$.
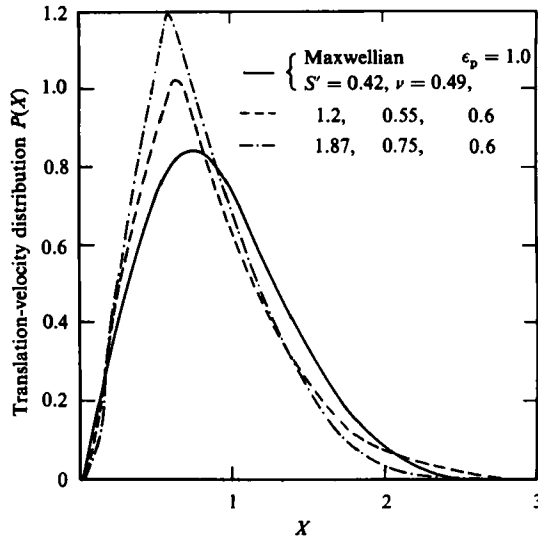
FIGURE 9. Translational-velocity distributions for type-B Couette-flow simulations.

indicate that the rotation is related to asymmetry in the stress tensor. The asymmetry disappears only if the rotation assumes a value on the order of $-\frac{1}{2}$ the local velocity gradient.

4. Velocity distribution functions

In drawing on the kinetic theory of non-equilibrium gases, the theoretical studies of Savage & Jeffrey (1981) and Jenkins & Savage (1983) assumed that the instantaneous particle velocities obeyed a Maxwell–Boltzmann velocity distribution about their mean values. (The gas temperature that normally appears in the Maxwell–Boltzmann expression was replaced with a measure of the random motions of the particles similar to that defined in (2).) This is quite a large assumption, because the derivation of the Maxwellian distribution assumed that the molecules interacted elastically under equilibrium conditions (i.e. no velocity, density or temperature gradients), far from the conditions present in granular flows.

The simulation's distributions of translational velocities u and v are shown in figure 9. The abscissa variable X is a measure of the deviation in the instantaneous velocity from its mean value, scaled by the component of the local temperature associated with the translational velocity components:

$$X = \left[\frac{(u-\langle u \rangle)^2 + v^2}{\langle u'^2 \rangle + \langle v'^2 \rangle}\right]^{\frac{1}{2}}. \tag{6}$$

The distribution is calculated by counting the number of particles possessing an instantaneous value of X that falls within a given range at each sampling time. After the sampling period the sums are normalized by dividing the total number of particles counted in each range by the total number of particles counted and the range width. The lines in figure 9 are drawn through the normalized sums.

In the type-B simulations, from which these curves are derived, the temperature and density is constant throughout the flow. The shape of the curve appears to depend only on the parameter S' defined above. For small values of S' the measured

distributions are indistinguishable from Maxwellians. (This is a two-dimensional Maxwellian, and has a slightly different shape from its familiar three-dimensional counterpart.) As S' increases, the distributions deviate, but still seem to retain the basic Maxwellian shape. From these and other distributions evaluated during the course of these investigations, it appears that the deviation depends only on S', and is independent of ν and ϵ_p. This is only true for type-B Couette flows. Distributions measured from type-A Couette flows and chute flows, which show temperature gradients and conduction effects, show much stronger deviations.

Other distributions for the individual velocity components and the 'total' distribution, which collectively describes rotational as well as translational velocities, were also measured and can be found in Campbell (1982). All the distributions show close to Maxwellian behaviour and deviate only with S and S'.

5. Comparison with existing constitutive models

In the absence of interstitial fluid, electrostatic or other effects, dimensional analysis requires that the stress tensor in a simple shear flow be given by

$$\sigma_{ij}^* = \rho_\mathrm{p} R^2 f_{ij}(\nu; \epsilon_\mathrm{p}) \left(\frac{\mathrm{d}u}{\mathrm{d}y}\right)^2, \qquad (7)$$

where ρ_p is the particle density and f_{ij} is some dimensionless tensor-valued function of ν and ϵ_p. This relation is supported by the Couette-flow experiments of Savage & Sayed (1980, 1983) and Bagnold (1954). (Bagnold's data have questionable relevance because of the unknown effects of the glycerol–water–alcohol mixture in which his particles were neutrally suspended.) Bagnold supported this model with a revealing heuristic argument. Almost all more exact calculations (e.g. McTigue 1978; Ackermann & Shen 1982; Jenkins & Savage 1983) lead to the same conclusion. Figure 5 demonstrates that such a relationship applies to the type-B Couette-flow simulations.

It seems questionable to try and adapt this model to other than simple shear flows (as did Savage 1979). In Bagnold's (1954) heuristic argument, one $\mathrm{d}u/\mathrm{d}y$ factor governs the interparticle collision rate, which controls the rate of momentum transport by collision. In a gas, the transport rate is governed by the gas temperature. Figure 5 shows that, for type-B Couette flows, $T \propto (RU/H)^2$, or $T^{\frac{1}{2}} \propto |\,\mathrm{d}u/\mathrm{d}y\,|$, from which it can be inferred that the temperature also governs the transport rate in granular flows. (As the viscosity of a Newtonian fluid is roughly proportional to the square root of its temperature, the expression above may be viewed as a self-excited Newtonian fluid with viscosity $\mu = \rho_\mathrm{p} R^2 f_{ij} |\,\mathrm{d}u/\mathrm{d}y\,|$.) However, there is no simple proportionality between the shear rate and temperature if there are gradients in the granular temperature (and the accompanying conduction effects) that were observed in non-simple shear flows such as chute flows and the type-A Couette flows. In such cases the constitutive behaviour should reflect the local granular temperature, which must be determined from a coupled granular energy equation that accounts for temperature conduction effects. (Jenkins & Savage (1983) present a granular energy equation, but do not apply it to situations with large temperature gradients.)

In a Couette-flow rheometer it is possible to measure the shear and normal stresses σ_{xy}^* and σ_{yy}^* on the solid walls, and from them to compute the corresponding values of f_{xy} and f_{yy}. These may be compared with similar measurement made on the type-B simulations. (The simulation wall stresses are defined as the time average of the impulses applied by particle–wall collisions.) Figures 10 and 11 show the values for f_{xy} and f_{yy} taken from simulations with $\epsilon_\mathrm{w} = 0.8$ and $\epsilon_\mathrm{p} = 0.6$. They are compared
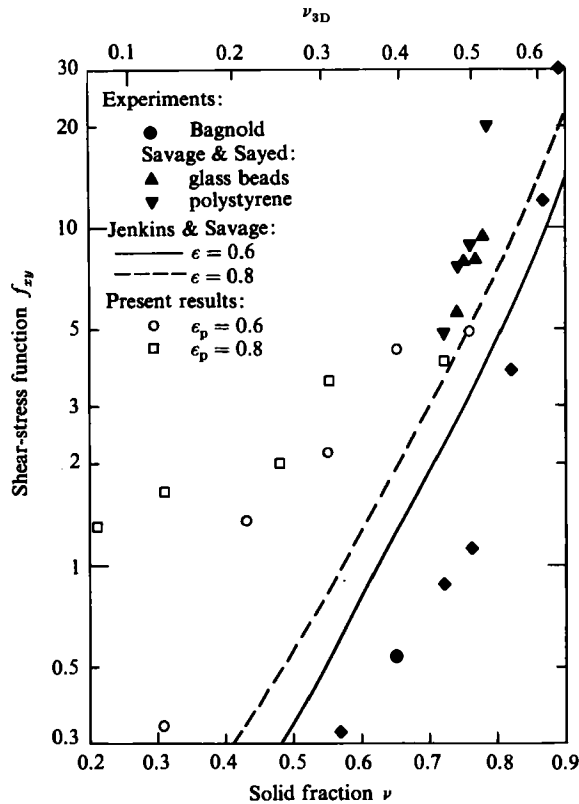
FIGURE 10. The shear-stress function $f_{xy}(\nu)$ for the type-B simulation, $\epsilon_w = 0.8$, compared with measured and predicted values.

with the experiments of Bagnold (1954) and Savage & Sayed (1980) (both sets of data were taken from Savage & Jeffrey 1981). The simulation results agree well with the measurements of Savage & Sayed (1980), but generally lie above Bagnold's results. (Some discrepancy would be expected owing to the low coefficient of restitution of Bagnold's wax spheres and the unknown effect of the viscous interstitial fluid.)

Also plotted are the corresponding curves predicted by Jenkins & Savage (1983). (Values of f_{xy} and f_{yy} are also predicted by Ogawa & Oshima (1977), Ogawa (1978), Oshima (1978, 1980) and Kanatani (1979a,b, 1980), but Savage (1984) shows that these are not in good agreement with the experimental results.) The values from the simulation agree with the predictions of Jenkins & Savage only at large values of the solid fraction. At lower solid fractions, the predictions fall well below the measurements. In their derivation Jenkins & Savage (1983) only consider momentum transfer by interparticle collisions. At large solid fractions this will indeed be the dominate transfer mechanism. However, at low solid fractions the 'kinetic' or 'streaming' mechanism of momentum transfer, akin to Reynolds stresses in turbulent fluid flow, becomes important, and, when added to the collisional contribution, could account for the observed discrepancy. (Furthermore, viscous interstitial fluid, used as a suspending medium in Bagnold's (1954) experiment, would damp the granular temperature and favour the collisional mode of momentum transfer. This is a partial explanation for the smaller values of f_{xy} and f_{yy} that Bagnold measured for low values of the solid fraction.)
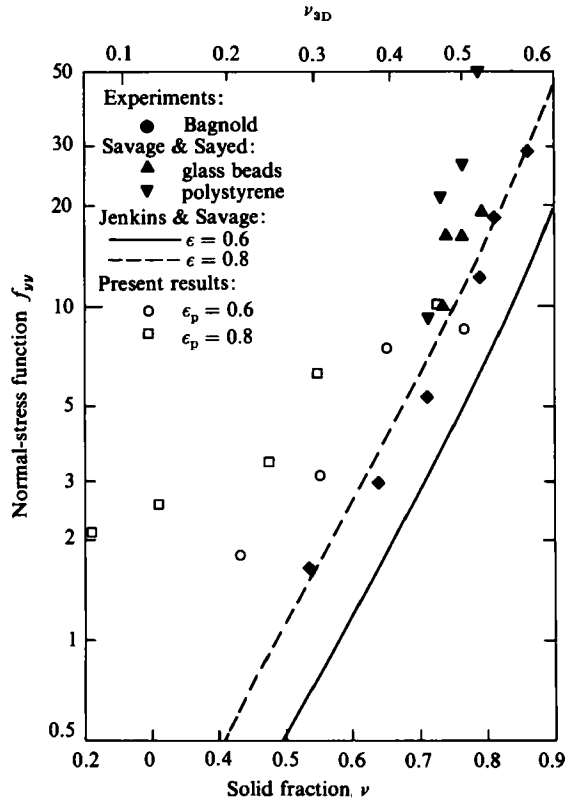
FIGURE 11. The normal-stress function $f_{yy}(\nu)$ for the type-B simulation, $\epsilon_w = 0.8$, compared with measured and predicted values.

It is difficult to compare the results of the two-dimensional simulation with the existing experimental and theoretical studies for spherical or near-spherical particles. To make the comparison shown in figures 10–12, we arbitrarily choose an equivalent three-dimensional solid fraction so that the average three-dimensional interparticle spacing $C = (4\pi/3\nu_{3D})^{\frac{1}{3}} R$ equals the average two-dimensional spacing $C = (\pi/\nu)^{\frac{1}{2}} R$. The equivalence is given by

$$\nu_{3D} = \frac{4}{3\pi^{\frac{1}{2}}} \nu^{\frac{3}{2}}. \tag{8}$$

In figures 10–12 the two-dimensional value ν is plotted on the lower abscissa, and the equivalent three-dimensional value ν_{3D} on the upper abscissa. Considering all the difficulties inherent in making a comparison, the simulation data agrees remarkably well with the experimental measurements.

Figure 12 is a plot of the friction coefficient σ_{xy}/σ_{yy} as a function of the solid fraction ν. Also plotted are experimental measurements on polystyrene beads from Savage & Sayed (1981 personal communication) and the values predicted by Jenkins & Savage (1983). Jenkins & Savage predict that the friction coefficient will depend only on the coefficient of restitution and will be independent of the solid fraction. Both the simulation and the experimental results show that the friction coefficient is a decreasing function of ν. (There is remarkably good agreement between the experiments and the $\epsilon_p = 0.6$ simulation.) This is a surprising result. A standard
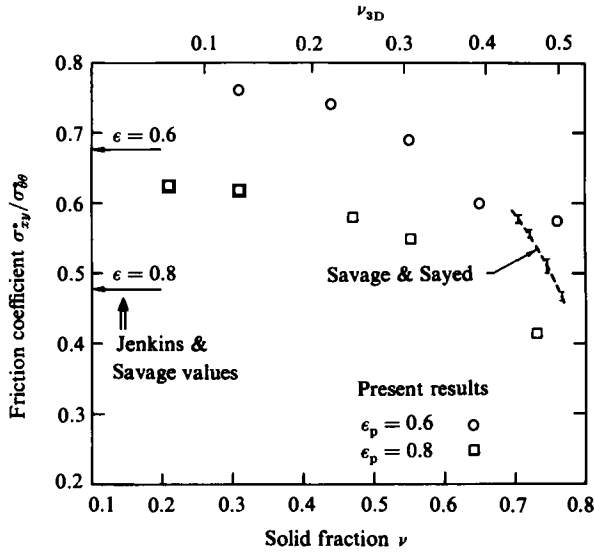
FIGURE 12. The friction coefficient σ_{xy}/σ_{yy} as a function of ν for the type-B simulations, $\epsilon_w = 0.8$. Also shown are the measurements of Savage & Sayed (1981) and the predictions of Jenkins & Savage (1983).

soil-mechanics test is to measure the yield strength of soils by shearing a static sample in a device similar to a Couette shear cell. The measurements always show that the yield strength increases with the packing of the sample. Apparently, the behaviour shown in figure 12 is a characteristic of fully developed granular flows. The effect can be attributed to variations in the collision-angle distribution, as will be described in §6.

6. The collision-angle distribution and the development of microstructure in flowing granular materials

As shown in figure 13(a), the collision angle θ is the inclination of a line connecting the centres of two colliding particles to the direction of mean flow. The collision angle will affect both the direction and magnitude of the impulse exerted during a collision. The 'continuum' stress tensor, exhibited by the bulk material, represents averages of collision impulses. Preferred values of θ could strongly affect the magnitude and relative magnitude of the stress-tensor components. The probability that a collision will occur at an angle is given by the collision-angle distribution $P(\theta)$, such that $P(\theta)\,\mathrm{d}\theta$ is the probability of a collision occurring in a neighbourhood of size $\mathrm{d}\theta$ about θ. ($P(\theta)$ may also be interpreted as a properly normalized angular distribution of collision frequency.) In a low-density uniform gas all collisions would be equally likely, or $P(\theta) = 1/\pi = \mathrm{const}$. Imposing a shear flow will induce an anisotropy into the distribution. Collisions are more likely to occur between particles whose relative velocities are augmented by gradients in the mean-velocity field; in a simple shear flow, as shown in figure 13(b), a particle is most likely to collide with the slower-moving particles in front of and below or be hit by the faster-moving particles from above and behind. This indicates a preference for collisions in the shaded regions of figure 13(b), which correspond to preferred collision angles in the range $0 < \theta < \frac{1}{2}\pi$. Savage & Jeffrey (1981) predict a collision pair-distribution function $g(\theta)$ (which may
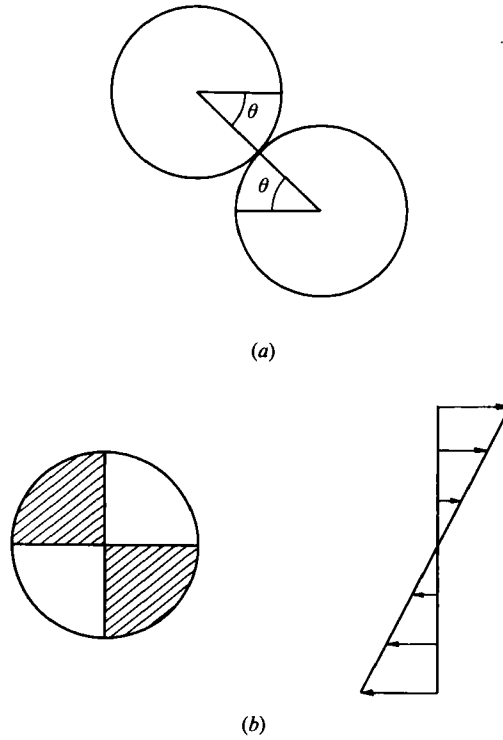
(a)

(b)

FIGURE 13. (a) Definition of the collision angle θ. (b) Collision
anisotropy induced by bulk shear motion.

be roughly interpreted as the probability that if two particles are in contact they will
lie at an angle θ). After conversion to two dimensions and normalizing, they predict

$$g(\theta) = \frac{1}{\pi} \, \mathrm{erfc} \, (2^{-\frac{1}{2}} S' \, \cos\theta \, \sin\theta), \tag{9}$$

where S' is as defined in (5) and erfc is the complementary error function. This
corresponds to a normalized collision-frequency distribution of the form

$$P(\theta) = A \, \mathrm{erfc} \, (2^{-\frac{1}{2}} S \, \sin\theta \, \cos\theta) \, [\exp(-\tfrac{1}{2} S'^2 \, \sin^2\theta \, \cos^2\theta)$$
$$- S' \, \sin\theta \, \cos\theta \, \mathrm{erfc} \, (2^{-\frac{1}{2}} S' \, \sin\theta \, \cos\theta)], \tag{10}$$

where A is a normalizing constant and is a function of S'. The values of $P(\theta)$, predicted
by (10), may be compared with collision-angle distributions measured directly from
the simulation. The distributions are measured in much the same way as the velocity
distribution, namely by counting the number of collisions that occur within small
ranges of θ. Figure 14 shows two collision-angle distributions that were measured in
low-density simulations. The corresponding curves are predicted by (10). Also plotted
are measured values of the collision pair-correlation function and the corresponding
theoretical curve of Savage & Jeffrey (1981) that is given in (9). Except for an angular
shift, the theoretical and measured curves show good agreement.

Figure 15 shows the collision-angle distribution $P(\theta)$ as a function of the density.
The distribution only has the form predicted by (10), at low densities. As the density
increases, a peak appears in the distribution about $\theta = 0$. The peak grows steadily
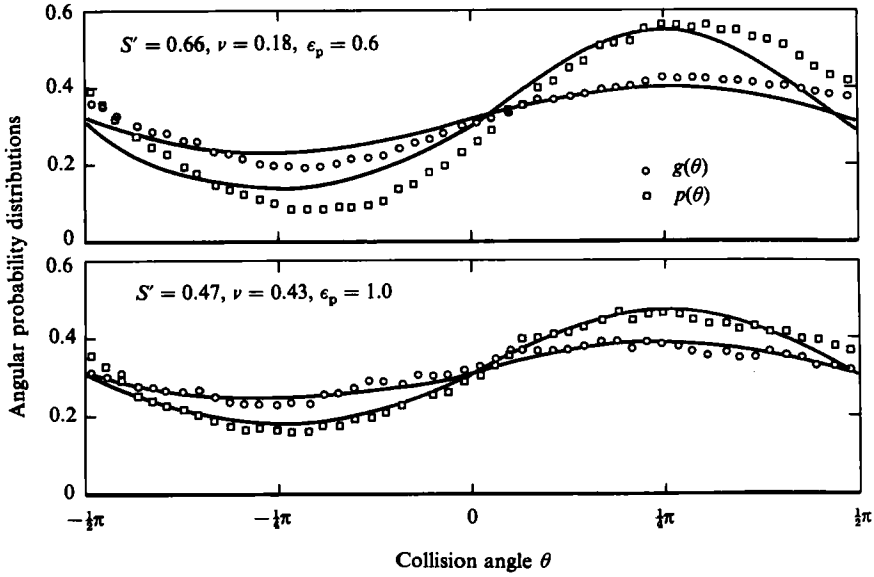with density until, at $\nu = 0.76$, the distribution consists only of a sharp peak about

FIGURE 14. Collision-angle distributions for two low-density simulations, $\epsilon_w = 1.0$. The solid lines are those predicted by (9) and (10).
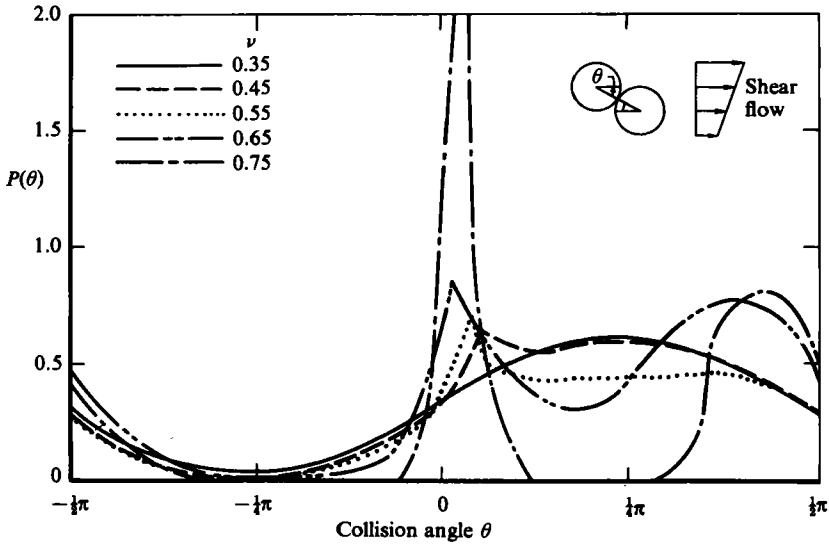

FIGURE 15. Collision-angle distributions for various solid fractions ν from type-B Couette-flow simulations, $\epsilon_w = 0.8$, $\epsilon_p = 0.6$.

$\theta = 0$ and a shorter, wider peak near $\theta = \pm\frac{1}{2}\pi$. The growth of the peaks accounts for the reduction in friction angle with density that was observed in figure 12. Collisions near $\theta = \pm\frac{1}{2}\pi$ are glancing blows, and the impulse applied by such a collision will have only a small component in the direction of flow. Averaging these impulses will result in reduced shear stresses and a consequent reduction in the friction coefficient. The peaks at both $\theta = 0$ and $\theta = \pm\frac{1}{2}\pi$ are reflections of a distinct microstructure developing within the flowing granular material. At high solid fractions the particles have restricted freedom of motion. A high-density shear flow may only be maintained if the particles align themselves into layers parallel to the flow direction. The layer

structure can be clearly seen in the snapshot in figure 2(c). The peak in $P(\theta)$ near $\theta = 0$ represents collisions between particles in the same layer, and the peak about $\theta = \pm\frac{1}{2}\pi$ represents collisions between neighbouring layers.

There are many possible internal structures for static granular assemblies. The layer formation and the corresponding anisotopy in the collision-angle distribution are properties of only fully developed granular flows and bear no relation to the mechanisms that determine the yield strength of a static material. Therefore it is not strange that the yield friction coefficient of a static sample increases with density while the flowing friction coefficient decreases.

The development of the layered structure can be observed in the simulation. The microstructure may be described by a 'pair-correlation function' denoted by $P(x, y \,|\, x_0, y_0)$ such that $P(x, y \,|\, x_0, y_0)\,dx\,dy$ is the probability of finding a particle centre in a neighbourhood $dx\,dy$ about (x, y) given that there is a particle centre already at (x_0, y_0). $P(x, y \,|\, x_0, y_0)$ represents the effect of a particle's position on the positions of its neighbours. (Naturally, for non-deformable solid particles of radius R, $P(x, y \,|\, x_0, y_0) = 0$ if $(x - x_0)^2 + (y - y_0)^2 < 4R^2$.)

These distributions are evaluated from the simulation by choosing a test particle (whose centre position determines (x_0, y_0)) and measuring the relative positions of the other particles. To reduce the effects of the solid walls, test particles are chosen to be every particle whose centre lies within a particle diameter of the midpoint between the solid walls – that is, $\frac{1}{2}H - 2R < y_0 < \frac{1}{2}H + 2R$. Because the periodic boundary condition imposes that there be no changes in the flow direction, and the density, temperature and velocity gradient are constant across the depth, $P(x, y \,|\, x_0, y_0)$ should be symmetric in both x and y.

In a shearing flow, particles in locations with different mean velocities (different y-coordinates) can have no correlations in the direction of flow (x-direction): the mean relative velocities will vary their relative x-positions continuously. The global pair correlation $P(x, y \,|\, x_0, y_0)$ may then be represented by two different probability distributions $P(|y - y_0|)$ and $P(|x - x_0|)$. $P(|y - y_0|)$ is the probability of finding a particle centre in the control volume at a vertical separation $|y - y_0|$ from the test particle. $P(|x - x_0|)$ is the probability of finding a particle centre with horizontal separation $|x - x_0|$ from the test particle provided that the particle's vertical coordinate lies within a particle diameter of the test particle's, i.e. $|y - y_0| < 2R$. (This is an approximation to the vertical range of influence of the test particle.) $P(|y - y_0|)$ will show the development of the layers across the depth, and $P(|x - x_0|)$ will show the development of structure within the layer.

Figures 16 and 17 show the measured values of $P(|y - y_0|)$ and $P(|x - x_0|)$. On the right-hand side of each plot is shown the number of particles per unit area, $n = \nu/\pi R^2$, which would be the expected values if the flow were undisturbed by the presence of the test particle.

At the lowest densities the only striking feature of the distributions is a small peak at a separation of $2R$. Beyond $2R$ the probability falls to the expected value. The primary influence of the test particle on its neighbours is to exclude their centres from lying within a particle diameter of the test particle's. Particles approach, collide with, and recoil from, the test particle. In doing so, they pass through roughly the same region twice and are double-counted by the distribution assessment, forming the peak at a separation of $2R$. As the density and the test particle's range of influence increases further, a second peak begins to form at a separation of $4R$. More peaks form with increasing density until, at the highest density, $\nu = 0.76$, the distribution is composed of very sharp peaks indicating well-developed layers. (The $\nu = 0.76$ distribution was
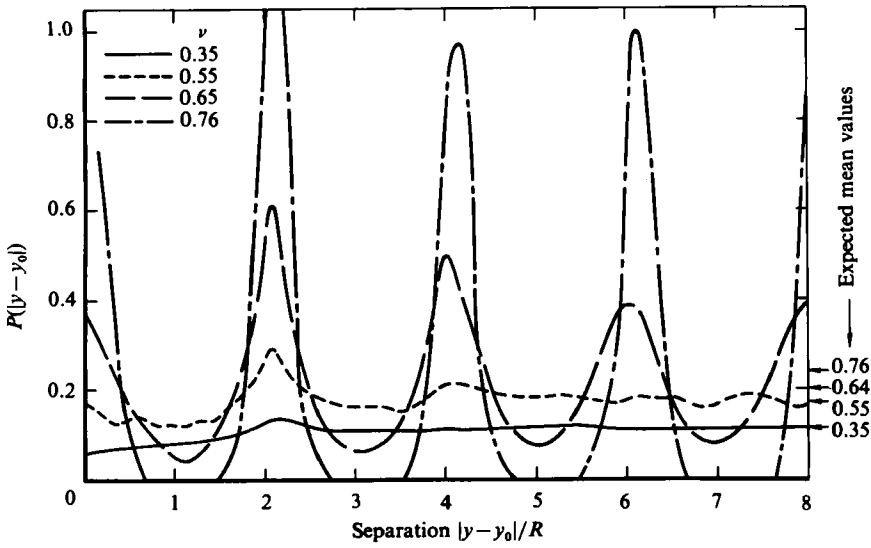
FIGURE 16. Normal pair-correlation $p(|y-y_0|)$, showing the formation of layers with increasing solid fraction, from the type-B simulations, $\epsilon_w = 0.8$, $\epsilon_p = 0.6$.
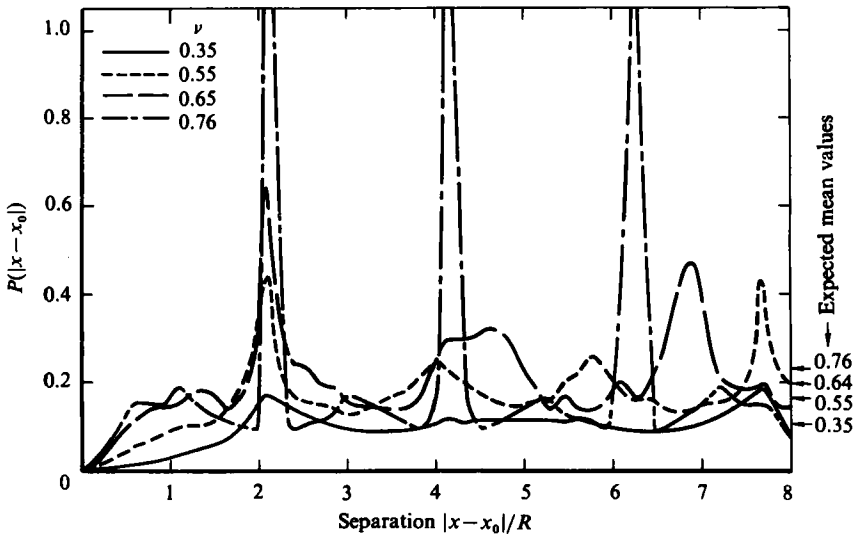

FIGURE 17. Parallel pair-correlation $P(|x-x_0|)$, showing the development of structure within a layer with increasing solid fraction, from the type-B simulatons, $\epsilon_w = 0.8$, $\epsilon_p = 0.6$.

measured from the same simulation that produced the snapshot, shown in figure 2 (c), in which the layered structure may be clearly seen.) One would expect that the development of layers would be slower in three-dimensional flows in which the particles are free to move normal to the shear plane.

7. Conclusions

A computer simulation has been developed that describes large deformations of granular assemblies. Once the mechanical system has been set up, 'experiments' are performed by averaging the system properties at successive sampling intervals. The

present form of the simulation describes two-dimensional unidirectional flows of inelastic fully rough disks. The simulation has been applied to gravity-driven inclined chute flows (the results of which are presented in Campbell & Brennen 1984) and the gravity-free flow in a Couette shear cell. Both models show good agreement with independent experimental measurements.

This paper reports the results of the Couette-flow calculations. Simulations were performed with two wall boundary conditions. The type-A or fully rough-surface condition assumes that after a collision there is zero relative velocity between the particle and wall surfaces. The generated velocity profiles show slip at both solid walls, and regions with large shear in the wall neighbourhood. Corresponding to the high-shear zones are regions of low density and large granular temperature.

After a collision with a type-B wall the particle's centre of mass assumes the wall's velocity. The generated velocity profiles vary linearly from zero at the stationary wall to the upper-wall velocity, and the density and temperature are nearly uniform across the depth. The angular rotation rate is also uniform across the depth and assumes a value of roughly half the mean shear rate. It is shown that, at constant density and in the absence of conduction effects, the temperature is proportional to the square of the shear rate. The ratio of shear rate to temperature represented by

$$S = \frac{2R \left| \dfrac{du}{dy} \right|}{T^{\frac{1}{2}}} \tag{11}$$

is shown to be an increasing function of solid fraction ν. The temperature is shown not to be equally partitioned between the three velocity components; the largest value is assumed by the temperature component in the direction of mean flow. Also the instantaneous particle velocities appear to obey very nearly a Maxwell–Boltzmann velocity distribution about their mean values.

The simulated wall stresses agree well with the results of the Couette-flow experiments of Bagnold (1954) and Savage & Sayed (1983) as well as the predicted profiles of Jenkins & Savage (1983). Furthermore, the wall-friction coefficient (the ratio of shear to normal wall stresses) was found to be a decreasing function of density. The same phenomenon is observed in the Couette-flow experiments of Savage & Sayed (1981, 1983) and run counter to the results of shearing static samples of material commonly performed for soil-strength testing. Observations from the simulation indicate that this effect is due to anisotropies in the collision-angle distribution which result from the development of a distinct microstructure within the material. A high-density shearing flow is only possible if the constituent particles are aligned into layers parallel to the direction of motion. The development of this layered microstructure within the simulated system has been explicitly shown.

REFERENCES

ACKERMANN, N. L. & SHEN, H. 1979 Stresses in rapidly sheared fluid–solid mixtures. *J. Engng Mech. Div. ASCE* **108**, 95–113.

BAGNOLD, R. A. 1954 Experiments on a gravity-free dispersion of large solid spheres in a Newtonian fluid under shear. *Proc. R. Soc. Lond.* A **225**, 49–63.

BAILARD, J. 1978 An experimental study of granular-fluid flow. Ph.D. thesis, University of California, San Diego.

BLINOWSKI, A. 1979 On the dynamic flow of granular media. *Arch. Mech.* **30**, 27–34.

CAMPBELL, C. S. 1982 Shear flows of granular materials. Ph.D. thesis (and *Rep.* E-200.7), Division of Engineering and Applied Science, California Institute of Technology.

CAMPBELL, C. S. 1984 Work in progress.

CAMPBELL, C. S. & BRENNEN, C. E. 1982a Computer simulation of shear flows of granular materials. In *Proc. 2nd US–Japan Seminar on New Models and Constitutive Relations in the Mechanics of Granular Materials, Ithaca, NY.* Elsevier.

CAMPBELL, C. S. & BRENNEN, C. E. 1982b Computer simulation of chute flows of granular materials. In *Proc. IUTAM Symp. on Deformation and Failure of Granular Materials, Delft, Netherlands.* Balkema.

CAMPBELL, C. S. & BRENNEN, C. E. 1984 Chute flows of granular material: some computer simulations, *Trans. ASME* E: *J. Appl Mech.* (to appear).

CHAPMAN, S. & COWLING, T. G. 1970 *The Mathematical Theory of Non-Uniform Gases*, 3rd edn. Cambridge University Press.

CUNDALL, P. A. 1974 A computer model for rock-mass behaviour using interactive graphics for input and output of geometrical data. *US Army Corps of Engrs (Missouri River Div.) Tech. Rep.* MRD-2074.

DAVIS, R. A. & DERESIEWICZ, X. X. 1977 A discrete probabilistic model for mechanical responses of a granular medium. *Acta Mech.* **26**, 69–89.

EINSTEIN, A. 1906 On the theory of the Brownian movement. *Ann. d. Phys.* **19**, 371–381. (English transl. in *Investigations on the Theory of the Brownian Movement.* Dover, 1956.)

FERZIGER, J. M. & KAPER, H. G. 1972 *Mathematical Theory of Transport Processes in Gases.* North-Holland.

ISHIDA, M. & SHIRAI, T. 1979 Velocity distributions in the flow of solid particles in an inclined open channel. *J. Chem. Engng Japan* **12**, 46–50.

JENKINS, J. T. & SAVAGE, S. B. 1983 A theory for the rapid flow of identical, smooth, nearly elastic particles. *J. Fluid Mech.* **130**, 187–202.

KANATANI, K. 1971a A micropolar continuum theory of granular materials. *Intl J. Engng Sci.* **17**, 419–432.

KANATANI, K. 1979b A continuum theory for the flow of granular materials. In *Theoretical and Applied Mechanics* (ed. Japan Natl Comm. for Theor. Appl. Mech.), vol. 27, pp. 571–578.

KANATANI, K. 1980 A continuum theory for the flow of granular materials (II). In *Theoretical and Applied Mechanics* (ed. Japan Natl Comm. for Theor. Appl. Mech.), vol. 28, pp. 485–497.

LANDAU, L. D. & LIFSHITZ, E. M. 1958 *Statistical Physics.* Pergamon.

McTIGUE, D. F. 1978 A model for stresses in shear flows of granular material. In *Proc. US–Japan Seminar on Continuum-Mechanical and Statistical Approaches in the Mechanics of Granular Materials*, pp. 266–271.

MROZ, A. 1980 On hypoelasticity and plasticity approaches to constitutive modeling of the inelastic behaviour of soils. *Intl J. Numer. and Anal. Meth. in Geomech.* **4**, 45–55.

OGAWA, S. 1978 Multi-temperature theory of granular materials. In *Proc. US–Japan Seminar on Continuum-Mechanical and Statistical Approaches in the Mechanics of Granular Materials*, pp. 208–217.

OGAWA, S. & OSHIMA, N. 1977 A thermomechanical theory of soil-like materials. In *Theoretical and Applied Mechanics* (ed. Japan Natl Comm. for Theor. Appl. Mech.), vol. 25, pp. 229–244.

OSHIMA, N. 1978 Continuum model of fluidized granular media. In *Proc. US–Japan Seminar on Continuum-Mechanical and Statistical Approaches in the Mechanics of Granular Materials*, pp. 189–202.

OSHIMA, N. 1980 Dynamics of fluidized granular material. In *Theoretical and Applied Mechanics* (ed. Japan Natl Comm. for Theor. Appl. Mech.), vol. 28, pp. 475–484.

SAVAGE, S. B. 1979 Gravity flow of cohesionless granular materials in chutes and channels. *J. Fluid Mech.* **92**, 53–96.

SAVAGE, S. B. 1984 The mechanics of rapid granular flows. *Adv. Appl. Mech.* **24**, 000–000.

SAVAGE, S. B. & SAYED, M. 1980 Experiments on dry cohesionless materials in an annular shear cell at high shear rates. Presented at Euromech 133 – Statics and Dynamics of Granular Materials, Oxford University.

SAVAGE, S. B. & SAYED, M. 1983 Stresses developed by dry cohesionless granular materials in an annular shear cell *J. Fluid Mech.* **142**, 391–430.

SPENCER, A. J. M. 1981 Deformation of an ideal granular material. In *Mechanics of Solids; Rodney Hill 60th Anniversary Volume* (ed. H. G. Hopkins & J. J. Sewell). Pergamon.

TROLLOPE, D. H. & BERMAN, B. C. 1980 Physical and numerical experiments with granular wedges. *Geotech.* **30**, 135–157.

WALTON, O. R. 1980 Particle dynamic modeling of geological materials. *Lawrence Livermore Lab. Rep.* UCRL-52915.

WALTON, O. R. 1982*a* Explicit particle dynamics model for granular materials. *Lawrence Livermore Lab. Rep.* UCRL-86260.

WALTON, O. R. 1982*b* Particle-dynamic calculations of shear flows. *Lawrence Livermore Lab. Rep.* UCRL-88560.